Talanta 113 (2013) 93–98

Contents lists available at SciVerse ScienceDirect

Talanta

journal homepage: www.elsevier.com/locate/talanta

Estimation with neural networks of the water content in imidazolium-based ionic liquids using their experimental density and viscosity values

José S. Torrecilla*, César Tortuero, John C. Cancilla, Pablo Díaz-Rodríguez

Department of Chemical Engineering, Complutense University of Madrid, E–28040 Madrid, Spain

ARTICLE INFO

Article history:
Received 13 December 2012
Received in revised form
18 March 2013
Accepted 25 March 2013
Available online 9 April 2013

Keywords:
Ionic liquid
Density
Viscosity
Water content
Relative humidity

ABSTRACT

A multilayer perceptron neural network (NN) model has been created for the estimation of the water content present in the following ionic liquids (ILs): 1-butyl-3-methylimidazolium tetrafluoroborate, 1-butyl-3-methylimidazolium methylsulfate, 1,3-dimethylimidazolium methylsulfate and 1-ethyl-3-methylimidazolium ethylsulfate. To achieve this goal, their density and viscosity values were used. The experimental values of these physicochemical properties, employed to design the NN model, were measured and registered at 298.15 K. They were determined at different relative humidity values ranging from 11.1 to 84.3%. The estimated results were then compared with the experimental measurements of the water content, which were carried out by the Karl Fischer technique, and the difference between the real and estimated values was less than 0.05 and 3.1% in the verification and validation processes, respectively. In addition, an external validation process was developed using four bibliographical references. In this case, the mean prediction error was less than 6.3%. In light of these results, the NN model shows an acceptable goodness of fit, sufficient robustness, and an adequate estimative capacity to determine the water content inside the studied range of the ILs analyzed.

1. Introduction

Room temperature ionic liquids (ILs) are low temperature molten salts which are formed by organic and inorganic ions. Since the possible combinations of anions and cations in ILs are very large, and the ions are weakly coordinated, these chemical compounds offer unique properties. In the past few years, ILs have become attractive candidates for replacing conventional organic solvents in several fields such as catalysis, separation processes, and petrochemistry [1–4]. Undoubtedly, in order to find and test new applications or design technical equipment, it is essential to know as many physicochemical properties of ILs as possible, such as their variation with temperature, pressure, or impurity contents.

It is well known that most ILs absorb water from wet surfaces or from the atmosphere [5,6]. This is relevant due to the fact that even low levels of water in ILs can dramatically alter their physical properties. Seddon et al. (2000) [5] and others [6–10] have previously studied the effect of water content on the density and viscosity of ILs. Given this influence, in order to maintain these properties in a suitable range, the design of a reliable method to determine the water content of the ILs is important. In a recent paper, the water content of five ILs was estimated using chaotic parameters calculated from the thermal degradation of ionic liquids using differential scanning calorimeter equipment and radial basis network [11]. As a continuation of that work, a simple method is proposed here. This method is based on the estimation of the water content in ILs by the measurement of two accessible properties, which are density and viscosity. The objective of this work is to design and test a multilayer perceptron neural network (NN, *vide infra*) model using density and viscosity values to estimate the water content in the following ILs: 1-butyl-3-methylimidazolium tetrafluoroborate ([bmim][BF_4]), 1-butyl-3-methylimidazolium methylsulfate ([bmim][$MeSO_4$]), 1,3-dimethylimidazolium methylsulfate ([mmim][$MeSO_4$]), and 1-ethyl-3-methylimidazolium ethylsulfate ([emim][$EtSO_4$]). In an attempt to design this mathematical tool, the NN model proposed has been internally validated using experimental measurements of density, viscosity, and water content. Additionally, this approach could lead towards the possibility of achieving an on-line control of the water content in ILs by measuring their density and viscosity.

2. Materials and methods

In this section, the databases and neural network used and all of necessary equipment and chemicals to measure density, viscosity, and water content of the aforementioned ILs are presented. These three properties have been modified changing the relative

* Corresponding author. Tel.: +34 91 394 42 44; fax: +34 91 394 42 43.
E-mail address: jstorre@quim.ucm.es (J.S. Torrecilla).

0039-9140/$ - see front matter © 2013 Elsevier B.V. All rights reserved.
http://dx.doi.org/10.1016/j.talanta.2013.03.060

Table 1
Purity, water, and halides mass fractions of the chemicals used.

Chemical	Purity mass fraction	Water mass fraction	Halides mass fraction	Supplier
[bmim][BF_4]	≥0.99	2.48×10^{-4}	$< 1 \times 10^{-4}$	IoLiTec
[mmim][$MeSO_4$]	≥0.99	1.84×10^{-5}	$< 1 \times 10^{-4}$	
[bmim][$MeSO_4$]	≥0.99	6.81×10^{-5}	$< 1 \times 10^{-4}$	
[emim][$EtSO_4$]	≥0.95	4.70×10^{-4}	$< 3 \times 10^{-5}$	Sigma-Aldrich Chemie GmbH
Lithium chloride	≥0.99			
Potassium acetate	≥0.99			
Magnesium chloride 6-hydrate	≥0.99			
Potassium carbonate	≥0.99			Panreac Chimie
Sodium dichromate 2-hydrate	≥0.995			S.A.R.L.
Sodium bromide	≥0.99			
Sodium nitrite	≥0.98			
Potassium chloride	≥0.9995			

Table 2
Solubility in water and relative humidity (RH) values generated inside the hydration equipment by saturated salt solutions at T=298.15 K at the equilibrium [13].

Chemical	Relative humidity (%)	Solubility (g/100 g)
Lithium chloride	11.1	84.8
Potassium acetate	22.5	269.5
Magnesium chloride	32.5	55.2
Potassium carbonate	43.7	112.5
Sodium dichromate	53.3	190.5
Sodium bromide	58.1	94.6
Sodium nitrite	64.4	84.2
Potassium chloride	84.3	35.7

humidity of air in a range of 11.1–84.3% at 298.15 K using salt solutions (*vide infra*).

2.1. Reagents, solutions, and instrumentation

2.1.1. Chemicals

Details of suppliers, water content, halides mass fraction, and purity of every compound used in this work can be found in Table 1. The aqueous solutions were prepared using ultra-pure water obtained from a Milli-Q water purification system (Millipore, Saint Quentis Yvelines, France).

All the samples of the ILs used were dried by heating them at 333 K for 24 h under reduced pressure (380 mmHg). All experiments were performed in a vacuum atmosphere glove box under dry nitrogen due to the highly hygroscopic nature of the ILs. Every sample was prepared in triplicate, and afterwards, viscosity and density were measured three times for each one. The water content of the samples was measured before and after each physicochemical property determination [6,7]. The non-IL compounds shown in Table 1 are used to create eight different relative humidity environments inside the hydration equipment described below.

2.1.2. Hydration equipment

In order to determine the absorption equilibrium moisture of [bmim][BF_4], [bmim][$MeSO_4$], [mmim][$MeSO_4$], and [emim][$EtSO_4$], an isopiestic method was used [12,13]. This method is used for equilibrating both the IL sample and the reference salt solutions (Table 2) in an evacuated desiccator until equilibrium is reached at 298.15 K. The water content of the reference material is then determined. The equipment and the experimental procedure were previously described in detail elsewhere [9]. For every IL used, several runs were developed in atmospheres with different air moisture values that were generated with the saturated solutions of different salts in water at 298 K and atmospheric pressure. The relative humidity (RH) values in the equilibrium of the eight saturated salt solutions at 298.15 K are listed in Table 2. Every IL was hydrated until the relative change of the water content rate, WCR (described by Eq. (1)), between two consecutive mass measurements of the container was ≤0.03% h^{-1}.

$$\mathrm{WCR} = \frac{\mathrm{Ms}(t+1) - \mathrm{Ms}(t)}{t\mathrm{Ms}_o} \times 100 \quad (1)$$

where Ms_0, Ms, and t are the initial sample mass, the sample mass as a function of time, and the hydration time in h, respectively. In this way, eight different hydrated solutions were made utilizing the eight respective saturated salts listed in Table 2 to hydrate the four ILs. When the water absorption equilibrium was reached, the physical properties of the ILs were measured (*vide infra*).

2.1.3. Density

The densities of the hydrated [bmim][BF_4], [bmim][$MeSO_4$], [mmim][$MeSO_4$], and [emim][$EtSO_4$] at 298.15 K and atmospheric pressure were determined using an Anton Paar oscillating U-tube density meter, model DMA 5000 (Anton Paar GmbH, Graz, Austria). The temperature was measured by using a Pt100 probe with a precision of ± 0.01 K. The uncertainty in the experimental measurements was less than $\pm 1 \times 10^{-5}$ g cm^{-3}. The density of ultra-pure water was determined using the same method, and the measurements are in agreement with the values found in the literature [14]. In addition, the density values for the pure ILs presented here also concur with published bibliographic values, Table 3.

2.1.4. Dynamic viscosity

Viscosities of hydrated [bmim][BF_4], [bmim][$MeSO_4$], [mmim][$MeSO_4$], and [emim][$EtSO_4$] were determined using an automated micro-viscometer, model AMVn (Anton Paar GmbH, Graz, Austria). The uncertainty in experimental measurements was less than ± 0.5%. The equipment accurately measures time and maintains the operating temperature of the capillary. The uncertainties were lower than 0.001 s and 0.01 K, respectively. The viscosity values reported in the literature for pure [bmim][BF_4], [bmim][$MeSO_4$], [mmim][$MeSO_4$], and [emim][$EtSO_4$] are in agreement with the data obtained in this work, Table 3 [15–17].

2.1.5. Water content

Determination of hydrated [bmim][BF_4], [bmim][$MeSO_4$], [mmim][$MeSO_4$], and [emim][$EtSO_4$] were performed utilizing a Karl Fischer titrator DL31 from Mettler Toledo and using the one-component technique. For volumetric Karl Fischer titration, dry methanol (CH_3OH, Riedel-de Haën, HYDRANAL-water mass fraction < 0.01%) and standard (Riedel-de Haën, HYDRANAL-standard (5.00 ± 0.02) mg mL^{-1} as water) were used. The polarizing current

Table 3
Comparison of measured pure component properties of [bmim][BF_4], [bmim][$MeSO_4$], [mmim][$MeSO_4$], and [emim][$EtSO_4$] (exp.) with literature values (lit.) at 298.15 K.

Ionic liquid	ρ/g cm^{-3}		η/mPa s	
	Exp.	Lit.	Exp.	Lit.
[bmim][BF_4]	1.2014	1.201[a] 1.20129[b]	104.91	103.9[b]
[mmim][$MeSO_4$]	1.3309	1.32725[c]	72.91	75.502[c]
[bmim][$MeSO_4$]	1.2225	1.20956[d] 1.21222[e]	194.23	213[e]
[emim][$EtSO_4$]	1.2363	1.23737[f]	91.85	95[f]

[a] [15].
[b] [16].
[c] [17].
[d] [18].
[e] [19].
[f] [7].

for the potentiometric end-point determination was 20 Å, while the stop voltage was 100 mV. The end-point criterion was the drift stabilization (3 μg $H_2O \cdot min^{-1}$) or maximum titration time (10 min). The measurement was corrected for the baseline drift, defined as the residual or penetrating water that the apparatus removes per minute. The uncertainty of the water content measurements estimated was lower than ± 2.5%.

2.2. Neural network model

The NN used here is a multilayer perceptron. It consists of several artificial neurons arranged in three layers (topology of NN): input, hidden, and output layers. The input layer is used to enter data into the NN; the nonlinear calculations are carried out in the other layers. The calculation process in each neuron of the hidden and output layers is done by successive activation and transfer functions. The goal of the activation function, Eq. (2), is to multiply the data inputted into each neuron by a self-adjustable parameter w, called weight; the result, x_k, is fed into a transfer function. The most common ones are the sigmoid, hyperbolical tangent, and linear transfer functions (TFs), Eqs. (3)–(5), respectively. The calculated value, y_k, is the output of the considered neuron.

$$x_k = \sum_{j=1} w_{jk} y_j \tag{2}$$

$$y_k = f(x_k) = \left(\frac{1}{1+e^{-x_k}}\right) \tag{3}$$

$$y_k = f(x_k) = \left(\frac{1-e^{-2x_k}}{1+e^{-2x_k}}\right) \tag{4}$$

$$y_k = f(x_k) = x_k \tag{5}$$

The learning process, which modifies the weights to improve the estimative capacity of the NN, takes place by minimizing a combination of squared errors and weights through the Bayesian regulation backpropagation (TrainBR) training function. This function uses the *Jacobian* for calculations, which assumes that the performance is a mean or sum of squared errors [20]. Using this method, the correct combination of weights is achieved, which in the end originates an optimized NN that is able to generalize correctly. TrainBR is a network training function that updates the weight and bias values according to the Levenberg–Marquardt optimization [20]. One of the most important features of the training function used here is that it provides a measure of how many network parameters (weights and biases) are being effectively employed by the network [20]. Since only the most important parameters of the NN are optimized, the number of data points required for the optimization process is reduced. Because of that, in the NN presented here, the overfitting effect is avoided and generalization capability is favored.

Apart from the weights, the NN has other parameters such as topology, Marquard adjustment parameter (learning coefficient, Lc), decrease factor for Lc (Lcd), and increase factor for Lc (Lci) [21]. Detailed information about these NN parameters can be found elsewhere [20]. The neural network used was designed with Matlab version 7.01.24704 (R14).

2.3. Learning, verification, and validation database

The databases employed to optimize the neural network used here have been obtained from the measurements of density, viscosity, and water content of every ionic liquid treated in this study. Experimentally, these three properties have been modified changing the relative humidity of air in a range of 11.1–84.3% at 298.15 K using the salt solutions shown in Table 2 and the isopiestic method (*vide supra*). As an example, some of the density and viscosity experimental values of [bmim][BF_4], [mmim][$MeSO_4$], and [bmim][$MeSO_4$], which were used in the learning and verification processes, *versus* the relative humidity of air and their water content are shown in Fig. 1.

The general database was divided randomly into three groups: learning, verification, and validation samples. The learning sample was used to optimize the model and the verification and validation databases were only utilized to evaluate its performance. The learning and verification datasets contain 80 and 10% of the general database, respectively. The validation samples contain the remaining 10% of the data points, Table 4. Acknowledging that the verification and validation sample ranges must be within the learning sample range, every data point of the general database was randomly distributed in order to create the verification and validation samples. In addition, to check the generalization capacity of the NN model, an external validation dataset has been defined and used to test it, Table 4. This dataset was obtained from different scientific references [17,22–24] and includes the water content values of [bmim][BF_4], [bmim][$MeSO_4$], [mmim][$MeSO_4$], and [emim][$EtSO_4$] measured at 298.15 K. These water content values are inside the learning sample range.

The learning, verification, and two validation datasets contain comparable information. In other words, every sample (IL) is defined by two independent variables (density and viscosity) and one dependent variable (water content). Table 4 presents the number of samples used for each type of IL in the learning, verification, and validation processes.

The applicability domain of the data used in the learning, verification, and validation samples has been evaluated following the calculation process described in the literature [25,26] which consists of determining the compounds with cross-validated standardized residuals greater than three standard deviation values. No anomalous dataset was found.

3. Results and discussion

The optimization, verification, and validation processes of the NN model applied to estimate the water content values (dependent variables) of the four studied ILs ([bmim][BF_4], [bmim][$MeSO_4$], [mmim][$MeSO_4$], and [emim][$EtSO_4$]) using their density and viscosity values as independent variables are described in this section.

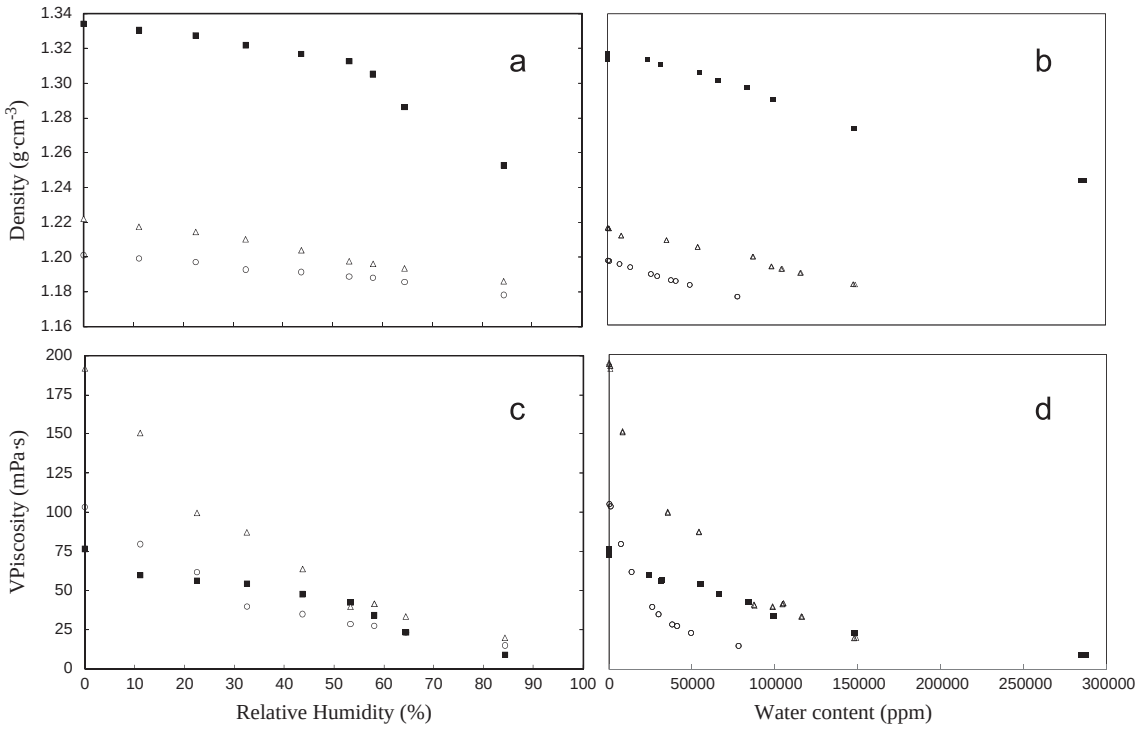

Fig. 1. Density (a and b) and dynamic viscosities (c and d) at 298.15 K of some of the ILs used *versus* relative humidity of air and water content in the ILs (○, [bmim][BF_4]; ■, [mmim][$MeSO_4$] and Δ, [bmim][$MeSO_4$]).

Table 4
Number of samples used in the learning, verification, and the two validation processes.

Ionic liquid	Number of samples				**Total**
	Learning	Verification	Internal validation	External validation	
[bmim][BF_4]	25	3	2	1[a]	**31**
[bmim][$MeSO_4$]	25	3	2	1[b]	**31**
[mmim][$MeSO_4$]	25	3	2	1[c]	**31**
[emim][$EtSO_4$]	28	4	4	1[d]	**37**
Total	**103**	**13**	**10**	**4**	**130**

[a] [22].
[b] [23].
[c] [17].
[d] [24].

3.1. Neural network model optimization

The design of the NN model required optimizing its parameters (topology, Lc, Lcd, and Lci). The NN used here is formed by three layers (input, hidden, and output), a topology extensively applied to solve numerous problems [21]. There are two nodes in the input layer which are used to introduce the density and viscosity values, and one neuron in the output layer to estimate the water content of every IL tested. The hidden neuron number (HNN) and other parameters of the NN have been defined by a series of optimization techniques (*vide infra*).

Regarding the training function, the TrainBR was selected because its generalization power is higher than other training functions, and additionally avoids overfitting when a small learning sample is used [20]. To avoid obtaining a NN model which overfits for the training dataset, the learning process was repeated while the verification mean square error, MSE, defined by Eq. (6), decreased. A detailed description of the calculation process is described in the literature [27].

$$\mathrm{MSE} = \frac{1}{N}\sum_{k=1}^{N}(r_k - y_k)^2 \quad (6)$$

In Eq. (6), N, y_k, and r_k are, respectively, the number of data points in the database, the response of the output neuron, and the corresponding real output response. The HNN and NN parameters are optimized in a single step using an experimental design based on the Box–Wilson Central Composite Design 2^4+Star Points. The experimental factors analyzed were Lc and Lcd (between 1 and 0.001) and Lci (between 2 and 100) [27]. Taking the learning sample size into account, the selected HNN range was from 2 to 15 [28]. The analyzed results of the experimental design were the mean prediction error (MPE), Eq. (7), which represents the verification prediction error, and

Table 5
Parameters of the neural network model and statistical results using the verification sample.

Parameter	Optimized values
Transfer function	Sigmoid
Training function	TrainBR
Hidden neuron number	7
Lc	0.55
Lcd	0.01
Lci	10
Statistical results	
MPE (%)	0.05
R_a^2	>0.99

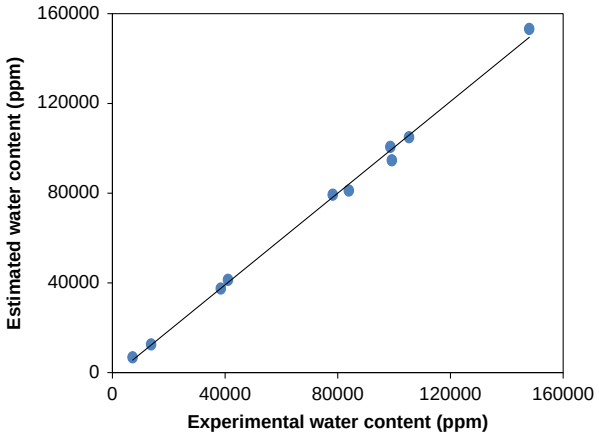

Fig. 2. Neural network model performances using the internal validation sample.

the adjusted correlation coefficient (R_a^2), Eq. (8). Both indexes are easily computed and provide a good description of the estimative performance of the network [29].

$$\mathrm{MPE} = \frac{1}{N}\sum_{k=1}^{N}\left|r_k - y_k\right| \tag{7}$$

$$R_a^2 = 1 - \frac{(1-R^2)(N-1)}{N-2} \tag{8}$$

where R^2 represents the correlation coefficient. Because the main goal is to have a NN that estimates results with the highest accuracy as possible, the considerations taken into account to analyze the experimental design were to obtain the least mean prediction error with the highest possible values of R_a^2.

Although a higher HNN implies a greater calculation complexity, considering that the water content of the four ILs should be estimated with the lowest performance error possible, a HNN equal to 7 was selected. The optimized parameters of the NN models are shown in Table 5. It is very troublesome to establish a relation between the optimal parameters and each system. It is important to highlight that the main objective during the design of a NN model is not to find the best model, but to find the model which best suits the user's requirements [30].

3.2. Application of the NN model

In order to carry out the validation of the optimized model, the aforementioned internal validation dataset was employed, Fig. 2. The mathematical procedure followed was similar to the verification process described above. The statistical results of estimated *versus* real values ($R_a^2 > 0.99$ and MPE $< 3.1\%$) are worse than those calculated in the verification process.

In addition, to check the generalization capacity of the NN model, an external validation dataset has been used. Four scientific references with information about the water content in four ILs and their respective density and viscosity values were studied [17,22–24] (*vide supra*). The independent variables have been inputted into the optimized NN model, and then the water content values have been estimated. The adjusted correlation coefficient and MPE were higher than 0.91 and less than 6.3% respectively. As it can be expected, these results are worse than the internal validation process mainly because the syntheses of these four ILs and the equipment employed for their analysis are different. Nevertheless, the results verify that these types of models are adequate to estimate the water content of these ILs. These statistical results are comparable with the estimations made with NNs based on chaotic parameters [11].

Taking into account the statistical results of the verification and validation processes, the optimized NN model has enough robustness and estimative capacity to determine the water content of these four ionic liquids using their density and viscosity values in the range of relative humidity employed (11.1–84.3% at 298.15 K).

4. Conclusions

In this work, the water content values of four imidazolium ionic liquids 1-butyl-3-methylimidazolium tetrafluoroborate, 1-butyl-3-methylimidazolium methylsulfate, 1,3-dimethylimidazolium methylsulfate, and 1-ethyl-3-methylimidazolium ethylsulfate have been estimated using their values of density and viscosity. The density, viscosity, and water content of the ILs have been modified changing the relative humidity of air in a range of 11.1–84.3% at 298.15 K. When the water absorption equilibrium was reached, these physical properties were measured. During the verification and internal validation processes, the water content was estimated with a MPE of less than 0.05 and 3.1%, respectively. In addition, in order to check the generalization capability of the optimized NN model, it has been tested using external databases from scientific references. In this case, although the statistical results were obviously worse (MPE $< 6.3\%$), the generalization capacity of the NN model was clearly observed. To sum up, after analyzing the obtained statistical results, this NN model shows an acceptable goodness of fit, sufficient robustness, and an adequate estimative capacity which allows the accurate determination of the water content present in the ionic liquids studied. Therefore, this approach could lead towards the possibility of achieving an on-line control of the water content in ILs by measuring their density and viscosity.

Acknowledgments

The research leading to these results has achieved funding from the European Union Seventh Framework Programme (FP7/2007–2013) under Grant Agreement no. HEALTH-F4-2011-258868.

References

[1] M. Freemantle, Chem. Eng. News 76 (1998) 32–37.
[2] R.D. Rogers, K.R. Seddon, Science 302 (2003) 792–793.
[3] N.V. Plechkova, K.R. Seddon, Chem. Soc. Rev. 37 (2008) 123–150.
[4] J.M. DeSimone, Science 297 (2002) 799–803.
[5] K.R. Seddon, A. Stark, M.J. Torres, Pure Appl. Chem. 72 (2000) 2275–2287.
[6] J.A. Widegren, A. Laesecke, J.W. Magee, Chem. Commun. (2005) 1610–1612.
[7] H. Rodríguez, J.F. Brennecke, J. Chem. Eng. Data 51 (2006) 2145–2155.
[8] A.M. O'Mahony, D.S. Silvester, L. Aldous, C. Hardacre, R.G. Compton, J. Chem. Eng. Data 53 (2008) 2884–2891.
[9] J.S. Torrecilla, T. Rafione, J. García, F. Rodríguez, J. Chem. Eng. Data 53 (2008) 923–928.

[10] P.J. Carvalho, T. Regueira, L.M.N.B.F. Santos, J. Fernandez, J.A.P. Coutinho, J. Chem. Eng. Data 55 (2010) 645–652.
[11] J.S. Torrecilla, E. Rojo, J.C. Domínguez, F. Rodríguez, Talanta 81 (2010) 1766–1771.
[12] W.A. Wink, Ind. Eng. Chem. Anal. Ed. 18 (1946) 251–252.
[13] J.S. Torrecilla, J.M. Aragón, M.C. Palancar, Eur. J. Lipid Sci. Technol. 108 (2006) 913–924.
[14] F. Sieweck, H. Bettin, Technisches Messen 59 (1992) 285–292.
[15] A. Soriano, B. Doma, M. Li, J. Chem. Thermodyn. 41 (2009) 301–307.
[16] K.R. Harris, L.A. Woolf, J. Chem. Eng. Data 50 (2007) 1777–1782.
[17] A.B. Pereiro, F. Santamarta, E. Tojo, A. Rodriguez, J. Tojo, J. Chem. Eng. Data 51 (2006) 952–954.
[18] A. Fernandez, J. Garcia, J.S. Torrecilla, F. Rodriguez, J. Chem. Eng. Data 53 (2008) 1518–1522.
[19] A.B. Pereiro, P. Verdia, E. Tojo, A. Rodriguez, J. Chem. Eng. Data 52 (2007) 377–380.
[20] H. Demuth, M. Beale, M. Hagan, Neural Network Toolbox for Use with MATLAB® User's Guide, Natick, Massachusetts, 2005, Version 4.0.6. Ninth printing Revised for Version 4.0.6 (Release 14SP3).
[21] J.S. Torrecilla, J.M. Aragon, M.C. Palancar, Ind. Eng. Chem. Res. 44 (2005) 8057.
[22] L.G. Sanchez, J.R. Espel, F. Onink, G.W. Meindersma, A.B. De Haan, J. Chem. Eng. Data 54 (2009) 2803–2812.
[23] B. Gonzalez, N. Calvar, E. Gomez, A. Dominguez, J. Chem. Thermodyn. 40 (2008) 1274–1281.
[24] E.J. Gonzalez, B. Gonzales, N. Calvar, A. Dominguez, J. Chem. Eng. Data 52 (2007) 1641–1648.
[25] P. Gramatica, QSAR Comb. Sci. 26 (2007) 694–701.
[26] P. Gramatica, E. Giani, E.J. Papa, J. Mol. Graph Model. 25 (2007) 755–766.
[27] J.S. Torrecilla, A. Fernández, J. García, F. Rodríguez, Ind. Eng. Chem. Res. 46 (2007) 3787–3793.
[28] Y. Sun, Y. Peng, Y. Chen, A.J. Shukla, Adv. Drug Delivery Rev. 55 (2003) 1201–1215.
[29] L.B. Sheiner, S. Beal, J. Pharmacokinet. Biopharm. 9 (1981) 503–512.
[30] A.A. Oliferenko, P.V. Oliferenko, J.S. Torrecilla, A.R. Katritzkya, Ind. Eng. Chem. Res. 52 (2013) 545–546.